AGU100 ADVANCING EARTH AND SPACE SCIENCE

Earth's Future

RESEARCH ARTICLE
10.1029/2018EF001007

Key Points:
- A midcentury (2042-2046) drought is simulated based on the record-breaking 2012-2016 California drought
- The modified thermodynamics from climate change greatly exacerbate the impacts of such a drought
- More frequent extreme heat, record-low snowpack, and extensive forest mortality are observed

Supporting Information:
- Supporting Information S1

Correspondence to:
P. Ullrich,
paullrich@ucdavis.edu

Citation:
Ullrich, P. A., Xu, Z., Rhoades, A. M., Dettinger, M. D., Mount, J. F., Jones, A. D., & Vahmani, P. (2018). California's drought of the future: A midcentury recreation of the exceptional conditions of 2012–2017. *Earth's Future*, *6*. https://doi.org/10.1029/2018EF001007

Received 8 AUG 2018
Accepted 20 SEP 2018
Accepted article online 28 SEP 2018

California's Drought of the Future: A Midcentury Recreation of the Exceptional Conditions of 2012–2017

P. A. Ullrich[1], Z. Xu[2], A.M. Rhoades[2], M.D. Dettinger[3], J.F. Mount[1,4], A.D. Jones[2], and P. Vahmani[2]

[1]Department of Land, Air and Water Resources, University of California, Davis, CA, USA, [2]Lawrence Berkeley National Laboratory, Berkeley, CA, USA, [3]U.S. Geological Survey, Carson City, NV, USA, [4]Public Policy Institute of California, San Francisco, CA, USA

Abstract The California drought of 2012–2016 was a record-breaking event with extensive social, political, and economic repercussions. The impacts were widespread and exposed the difficulty in preparing for the effects of prolonged dry conditions. Although the lessons from this drought drove important changes to state law and policy, there is little doubt that climate change will only exacerbate future droughts. To understand the character of future drought, this paper examines this recent drought period retrospectively and prospectively, that is, as it occurred historically and if similar dynamical conditions to the historical period were to arise 30 years later (2042–2046) subject to the effects of climate change. Simulations were conducted using the Weather Research and Forecasting model using the pseudo global warming method. The simulated historical and future droughts are contrasted in terms of temperature, precipitation, snowpack, soil moisture, evapotranspiration, and forest health. Overall, the midcentury drought is observed to be significantly worse, with many more extreme heat days, record-low snowpack, increased soil drying, and record-high forest mortality. With these findings in mind, the data sets developed in this study provide a means to structure future drought planning around a drought scenario that is realistic and modeled after a memorable historical analog.

Plain Language Summary The California drought of 2012–2016 was notorious for breaking numerous temperature, precipitation, and snowpack records. However, it was also a warning of the types of droughts we are likely to experience in light of climate change. In order to better understand and quantify the characteristics of future drought in California, this study uses a climate modeling technique known as pseudo global warming to simulate a midcentury (2042–2046) drought that is realistic in light of this recent historical analogue. Overall, the midcentury drought is much worse than its historical counterpart, with many more extreme heat days, record-low snowpack, increased soil drying, and record-high forest loss. This study points to the extensive effort that must now be invested on the part of California's residents, water managers, policymakers, and the broader stakeholder community to prepare for the next big drought.

1. Introduction

Global climate change is actively altering the Earth system, pushing up temperatures and producing shifts in precipitation patterns and intensity (Trenberth, 2011). These shifts drive indirect impacts, such as increased frequency and intensity of heat extremes, more widespread wildfires, increased snowpack loss, and increased propensity for drought conditions. Therefore, the development of a coordinated response to these changes is one of the most pressing challenges of the coming century.

In order to support drought adaptation planning, this paper describes a possible midcentury drought in California and Nevada produced using the pseudo global warming method (Kimura & Kitoh, 2007). Our drought scenario covers the period of 2042–2046 and is modeled closely off of the recent and record-breaking drought of 2012–2016, modified to account for anticipated changes in global climatology that will arise because of shifts in atmospheric temperatures, sea surface temperatures, and humidity through midcentury. Our hypothetical drought retains the basic meteorological character of the 2012–2016 drought, including the timing of storm events and heat waves through this period. Further, we include the 2017 water year (WY) in our assessment, which was a record-breaking year for precipitation acting as a *drought buster*.

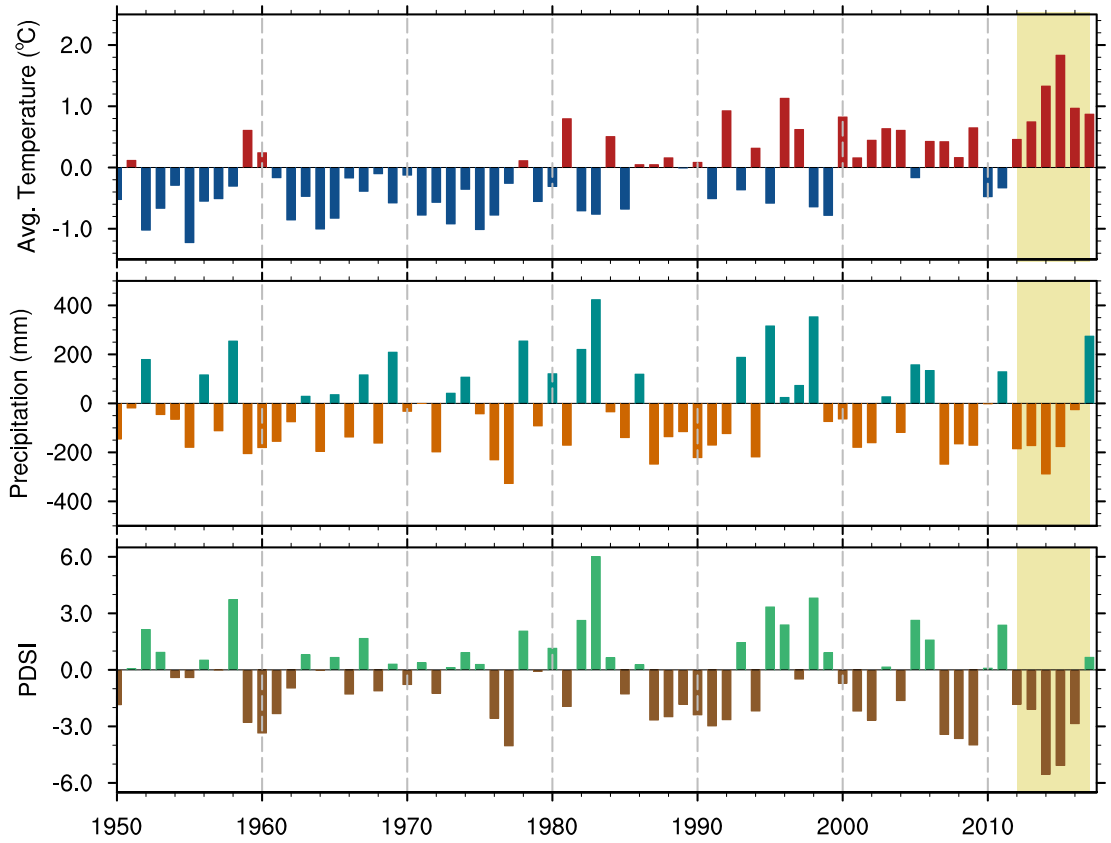

Figure 1. California water year climatological temperature anomaly, precipitation anomaly, and Palmer Drought Severity Index (PDSI) over the period WY1950 to WY2017. Temperature and precipitation anomalies are computed against 1981–2000 annual mean of 14.6 °C and 603 mm, respectively. The drought period considered in this paper is highlighted. Data from National Oceanic and Atmospheric Administration (2018).

The focus of this study is on California's Central Valley and the rugged mountains of the Sierra Nevada, two regions integral to the State's thriving economy. The former region is at the heart of California's agricultural industry, which produces more than 55% of the nation's fruits, nuts, and vegetables and is the national leader in dairy production (California Department of Food and Agriculture, 2016). The latter region supports the vast coniferous forests of California and is the source of two-thirds of the State's surface water use, largely through seasonal mountain snowpack (Hanak et al., 2017). Rising temperatures and changes to water availability in these regions have the potential to greatly increase stress on forests and crops, impact the working conditions of farm communities, and alter the magnitude, phase, and timing of the water supply.

The results of this study highlight some of the fundamental challenges for California in the coming century. As a direct consequence of climate change, substantially higher temperatures are expected throughout the region, particularly at higher elevations and through the winter season. We observe that summertime warming leads to more frequent extreme heat days, while higher wintertime temperatures reduce snow accumulation and shorten the snow season length. Examining shifts in precipitation amount, our results suggest that *wet becomes wetter* and *dry becomes drier* (Held & Soden, 2006)—precipitation becomes increasingly concentrated in the northern portion of the State during the winter season, accompanied by enhanced drying through the dry season and in Southern California. As a result of reduced snow water and a shorter snow season length, summertime soil drying is observed to occur largely at higher elevations with little change in the summertime soil moisture of the Central Valley. Evapotranspiration (ET) remains largely steady or increases throughout California, but substantial decreases are felt in summertime in the mountains due to soil drying. To further assess mountain forest viability under the midcentury drought, forest drought stress index (FDSI) was calculated and observed to reach previously unseen levels in the future drought. Overall, these results suggest that a midcentury drought similar to the recent drought would further exacerbate adverse conditions related to water availability, human health, and natural ecosystems.

The structure of this paper is as follows. The historical drought period is described in terms of its climatology and impacts in section 2. The outlook for future drought periods of similar character is then discussed in section 3. Our future drought scenario is then described and contrasted with the historical drought period in section 4. Finally, major findings and conclusions are given in section 5.

2. California's 2012–2017 Period in Retrospect

Droughts in California, defined by anomalously low soil moisture and available water, are triggered by a dearth of wintertime storms and exacerbated by high temperatures. Among the many historical droughts in California, the 2012–2016 drought was notable for its record-high temperatures and extreme precipitation deficits (Figure 1). However, this period was also associated with sequential years of substantially different hydroclimatological character. Before proceeding, we assess this drought in retrospect and review the key drivers and impacts from each WY of the drought.

Leading into the drought period, California had just experienced a particularly wet year in WY2011, and California's surface reservoir volume was above its historical average. WY2012 and WY2013 were fairly nominal examples of dry years in California but were important for priming the State for its descent into the drought—by the end of WY2013, surface reservoir levels had fallen to approximately 78% of historical. The first year of abnormal drought conditions was WY2014, characterized by record-high dryness driven by what is now colloquially referred to as *the Ridiculously Resilient Ridge*, a region of anomalously persistent blocking that redirected atmospheric moisture northward and led to record-high precipitation through the Pacific Northwest and Alaska (Swain et al., 2014). Drought conditions were further worsened by extreme temperatures during WY2014 that were the highest recorded since official records began in WY1896. Consequently, the Palmer Drought Severity Index (PDSI; Palmer, 1965), a commonly employed mechanism for monitoring drought intensity, reaching a record-low value of −7.01 in July 2014, indicative of extraordinary drought conditions.

WY2015 was again associated with anomalously low precipitation, consistent with precipitation amounts received in WY2012 and WY2013. However, drought in this period was particularly extraordinary because of anomalously high temperatures that broke the records set only a year earlier (December-January-February average 3.6 °C or 6.5 °F above the twentieth century mean). The combination of low precipitation and extraordinarily high temperatures led to the lowest snowpack on record (5% of normal for 1 April). This period has since become exemplary of a *snow drought* (Harpold et al., 2017).

Predictions of extremely strong El Niño conditions in WY2016 provided some hope for relief from the extreme drought conditions that continued to afflict Southe rn California. However, the El Niño that emerged was unusual as it actually enhanced total precipitation in Northern California instead, as a consequence of a northward shifted and intensified storm track that accompanied a positive geopotential height anomaly off the California coast (Paek et al., 2017; Wang et al., 2017). Against expectations, the drought was exacerbated throughout Southern California and produced record rainfall throughout parts of the Pacific Northwest (National Oceanic and Atmospheric Administration/National Centers for Environmental Information, 2018).

The prolonged dry period finally came to an end in WY2017, a year characterized by record-breaking precipitation, an above-average count of atmospheric rivers, and high levels of snowpack. Consequently, this year was widely referred to as a drought buster (Dettinger, 2013) and led to most of California's critically dry reservoirs being quickly replenished. Over much of the 2016–2017 winter season, a semipersistent jet stream pattern was present that consistently directed storms toward California (Wang et al., 2017). The meteorological conditions of this year contrasted starkly with the persistent pattern present during the 2012–2016 drought. Notably, the unusual wetness of this period was associated with a near-average El Niño Southern Oscillation.

Over the period WY2012–2015, the accumulated precipitation deficit across California was greater than 100% to 180% of the historical average annual precipitation total. Under these dire precipitation conditions, California's reservoirs, snowpack, rivers, vegetation, and groundwater all suffered considerably. Several different measurements of change in overall water content in the Central Valley and surroundings indicated that the net water loss totaled somewhere between 500 mm (Borsa et al., 2014) and 2,000 mm (Scanlon et al., 2012) in drought years when compared with annual average precipitation totals (750 mm). Hydropower generation in California between 2012 and 2015 was about 1.5 GW/year below normal, and freshwater outflow through the Sacramento-San Joaquin Delta totaled 24 million acre-feet (1 MAF = 1.23348 km^3) below normal overall (California Department of Water Resources, 2018a; California Energy Commission, 2018). The forests of the

Sierra Nevada struggled with the widespread declines in soil-water availability, with estimates of more than a 30% reduction in canopy water (a measure of drought stress on forests) in large trees within 1×10^6 ha of the range's forests by the end of 2015 (Asner et al., 2015). By end of 2016, the U.S. Forest Service reported that 102 million trees had died across California, with 62 million dying in 2016 alone. Meanwhile, with curtailment of surface water rights and deliveries imposed by 2015, including even the most senior rights in the Sacramento Valley, groundwater pumpage was estimated to have increased to 125% or more of recent (pre-2011) norms as an alternative water source. These increases in pumpage exacerbated aquifer overdraft conditions in many areas, including most notably the Central Valley where overdrafts resulted in lower groundwater levels, land subsidence, and water quality problems.

This drought period was not an isolated event but rather embedded within a drier-than-not period that began in around 1999 (Figure 1). This longer period has been characterized by low State-wide precipitation, with brief interruptions, along with drier overall conditions than the preceding several decades as shown in the long-term PDSI. Historically, drought has always been a regular part of California's landscape. But a dry period as extended and severe as this recent period severely challenged California's reservoirs and capacity to meet water demand. Thus, this drought needs to be understood as part of a longer, larger, and even more complex episode in California's history and future.

3. Future Outlook for Drought in California

Much like any single meteorological event, the cause of the 2012–2016 California drought is not rooted in one mechanism but arose from a pattern of dynamical and thermodynamical anomalies. With that said, significant evidence has emerged to support the role of anthropogenic climate change in enhancing and modifying these patterns into the future (AghaKouchak et al., 2014; Funk et al., 2014; Swain et al., 2014; Wang et al., 2014). As temperatures rise in response to increasing greenhouse gas concentrations in the global atmosphere, California's hydroclimatic regimes—including its droughts—are projected to change (Cook et al., 2015; Swain et al., 2018).

Dynamically, the drought period was characterized by persistent high-pressure ridging in the eastern Pacific that peaked in intensity in 2014. High-pressure ridges of this sort are associated with a clockwise circulation pattern that redirect storms northward, leading to enhanced precipitation in the Pacific Northwest and along the Alaskan Coast and dry conditions in California. Such patterns are connected with midlatitudinal atmospheric dynamics, although there is evidence to suggest that these wintertime patterns are exacerbated by anomalous tropical heating patterns (Teng & Branstator, 2017) and variations in Arctic sea ice extent (Cvijanovic et al., 2017; Sewall & Sloan, 2004). Funk et al. (2014) noted that the unprecedented intensity of the geopotential height was unlikely without accounting for anthropogenic climate change, with extreme ridging being predicted to become more frequent under future climate change (Swain et al., 2014).

Thermodynamically, the drought period was characterized by exceptionally high temperatures that were persistent and far above the norm for the twentieth century coupled with abnormally low precipitation totals. Williams et al. (2015) claimed that anthropogenic climate change enhanced the summertime PDSI through the drought period by 8–27% in 2012–2014 and 5–18% in 2014 alone. In response to anthropogenic warming, California's air temperatures are projected to warm by between 1.4 and 6 °C by end of century, depending on the climate model and greenhouse gas emissions used (e.g., California Climate Change Technical Advisory Group (CCTAG), 2015); these warmer temperatures are generally expected to decrease relative humidity over land, decrease soil moisture, increase ET, and reduce snowpack in ways that will mirror, and likely exceed, the temperature impacts in this current drought.

Although the past two decades have emerged as unusually dry in California's recorded history, there is little evidence of a historical trend in WY precipitation totals. Similarly, climate model projections of statewide precipitation amounts that account for future anthropogenic climate change largely disagree on the sign of the change (e.g., CCTAG, 2015)—likely indicative that the magnitude of the change will be small. With that said, there is some agreement that precipitation over southern California will modestly decline as part of the general spread and intensification of the global subtropical desert belts. These same model results produce a mixture of changes in ridging frequency, increased numbers of atmospheric rivers (in most models), a more variable jet stream (with low levels of model-to-model consensus), and El Niño Southern Oscillation changes (with, as yet, much divergence among models). For example, while models show little consensus as to the future of the frequencies of El Niños, projections are more consistent at indicating an increased likelihood of

very strong El Niños going forward (Cai et al., 2014). With that said, the events of 2016 have shown that even strong El Niños have only a probabilistic, and uncertain, influence on California's precipitation.

Although future mean annual statewide precipitation totals are poorly constrained, more can be said about precipitation character. Recent analyses of the current generation of climate-change projections indicate that (a) in essentially all models, the number of dry days per year are projected to increase significantly in response to changes in atmospheric circulation patterns (e.g., Prein, Holland, Rasmussen, Clark, and Tye (Prein et al., 2016) and a relatively dry atmosphere over California (Polade et al., 2014), but (b) in most models (80% in some studies), the intensity of the largest storms is projected to increase (Dettinger et al., 2016; Pierce et al., 2013) in response to the greater vapor-holding capacity of a warmer atmosphere. Trends in the intensity and frequency of storms weaker than these largest storms are not consistent among current models. This provides us with a picture of California's future climate as being drier most of the time, punctuated by occasional larger storms.

Between the warming, warming effects, and changes in precipitation patterns, droughts are expected to become more prevalent and more intense overall. For example, Cook et al. (2015) evaluated droughts in projections by 17 climate models and found that the risk of a recurrence of drought conditions of a decade or longer with the severity of megadroughts from the medieval period in California and the Southwest increases substantially from <12% historically to >80% by end of century, depending on which greenhouse gas emission scenario prevails. Building on current climate projections, Ault et al. (2014) also estimated that the risk of a decadelong megadrought this century is at least 80%, and the risk of even longer droughts is substantial, for example, as much as 50% for droughts up to 35 years in length and 5–10% for a 50-year drought in response to continuing and rapidly increasing greenhouse gas emissions.

4. A Midcentury Drought in California

In order to better understand the impact of anthropogenic climate change on drought in California, this study assesses how a midcentury (2042–2046) drought would differ if the same dynamical conditions emerged as those for the 2012–2016 drought. In our modeled midcentury drought, only temperature, greenhouse gas concentrations, and sea surface temperatures have been modified from their historical values, allowing us to isolate how future trends in the thermodynamics of the environment will affect the local climatology. This technique, dubbed pseudo global warming (Kimura & Kitoh, 2007), allows us to avoid biases that are well known among general circulation models when projecting changes in atmospheric dynamics.

4.1. Methodology

The Weather Research and Forecasting (WRF) Model (Skamarock et al., 2005) is one of the most widely used regional climate models and features multiple options for boundary layer, convection, microphysics, radiation, and several land surface model choices. In this study, the WRF-ARW version 3.8 modeling system is used. The two simulation periods are henceforth referred to as historical (1 June 2012 to 30 September 2017) and projected (1 June 2042 to 30 September 2047). WRF has been previously assessed for modeling California's climate and has been shown to provide an accurate representation of temperature, precipitation, and snowpack (Caldwell et al., 2009; Huang et al., 2016; Rhoades et al., 2016). Two land surface models were compared: the default Noah land model and the Community Land Model (CLM). In both simulations the land and atmosphere models were fully coupled. Overall, the WRF-CLM simulation was more consistent with historical observations and so was chosen for use in this study. Lateral forcing for the historical period was imposed from the 6-hourly National Center for Environmental Prediction Final global reanalysis at 1° resolution (Kalnay et al., 1996). Lateral forcing over the future period was identical to the historical reanalysis except for a modified time-dependent vertical temperature profile; that is, wind speed and relative humidity were held constant (each as a function of the vertical pressure coordinate). The temperature delta was applied uniformly along all boundaries and chosen in accordance with monthly projected temperature differences from the Coupled Model Intercomparison Project (CMIP5) under Representative Concentration Pathway (RCP) 8.5 (see supporting information); its value is positive at the near-surface (0.83–1.34 °C), increases with altitude to a maximum at ~400 hPa (1.58–2.03 °C), then decreases, reaching negative values above ~100 hPa (~ −2.4 °C at 10 hPa). Among CMIP5 models, the ensemble mean relative humidity in the eastern Pacific shows essentially negligible change between historical and midcentury periods, so it is assumed constant for our purposes. Note that the assumption of constant relative humidity in conjunction with increased temperatures implies higher overall atmospheric water vapor content. Sea surface temperatures were also adjusted in accordance with monthly

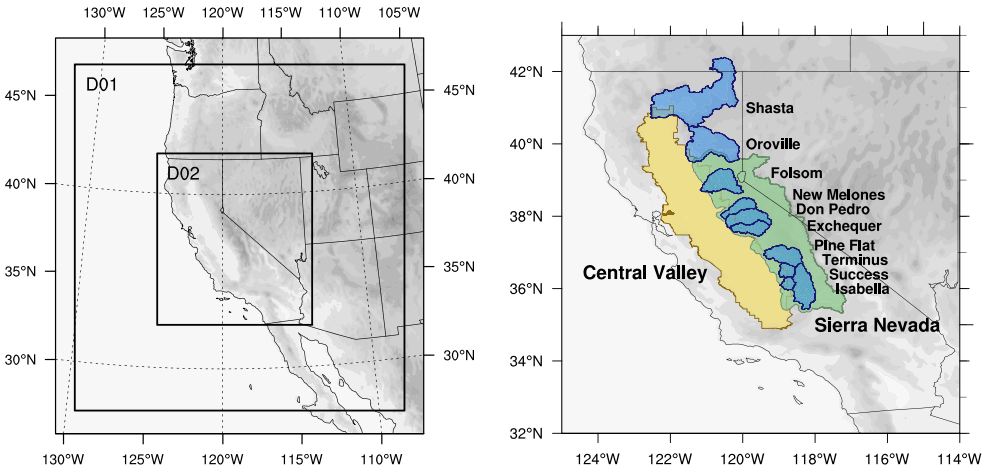

Figure 2. (left) The nested Weather Research and Forecasting domains used for this study; domains D01 and D02 are simulated with a grid spacing of 27 km (1/4°) and 9 km (1/12°), respectively. (right) Named analysis regions used in this study.

differences obtained from CMIP5 models when comparing the projected and historical periods. Atmospheric greenhouse gas concentrations, used in the radiation parameterization, are modified in accordance with the RCP8.5 scenario.

The two WRF nested domains are centered on California (Figure 2). The outer and inner domains are set at 27 and 9 km, with 75 × 80 and 105 × 120 grid points in the zonal and meridional directions, respectively. Ten grid points are used for relaxation to the coarse solution in each domain; spectral nudging is not used in this study. The 30-arc second (~ 1 km) resolution United States Geological Survey-based land use and land cover and topography data sets are interpolated to model grid points to obtain grid point elevations for WRF. The physical parameterizations employed for historical and projected simulations are described in Table 1. Simulation data are available from Ullrich et al. (2018). Climatological validation of near-surface temperature and precipitation fields was performed and described in the supporting information.

4.2. Temperature

Figure 3 depicts the seasonally averaged daily 2-m temperature over the winter months (December-January-February) and summer months (June-July-August, JJA). Note that the modified near-surface lateral boundary conditions and sea surface temperatures that emerged from CMIP5 models were approximately 1 °C higher through midcentury; hence, it is not surprising to see an analogous increase in projected temperatures, particularly along the western edge of the domain. However, we do see enhanced temperatures (on the order of 1.5 °C) in the Sierra Nevada and the drier parts of the domain. Throughout these regions near-surface humidity and soil moisture is insufficient to buffer the warmer temperatures. A pronounced elevation-dependent warming signal is seen (Pepin et al., 2015; Figure 4a), which emerges because of the increase with altitude of the temperature delta and loss of soil moisture at higher elevations (see section 4.5). However, this change is further enhanced in the winter season as a result of surface warming triggered by a loss of snowpack at higher elevations (see Figure 4b), namely, through snow-albedo feedback. Consequently,

Table 1
Physical Parameterizations Employed for the WRF Simulations Analyzed in This Paper

Process	Parameterization
Microphysics	CAM V5.1 two-moment five-class (Neale et al., 2010)
Radiation	RRTMG (Iacono et al., 2008)
Surface layer	Revised MM5 similarity theory (Jiménez et al., 2012)
Land surface model	CLM4 (Oleson et al., 2010)
Planetary boundary layer	UW (Bretherton & Park, 2009)
Cumulus parameterization	Zhang and McFarlane (1995)

Note. WRF = Weather Research and Forecasting.

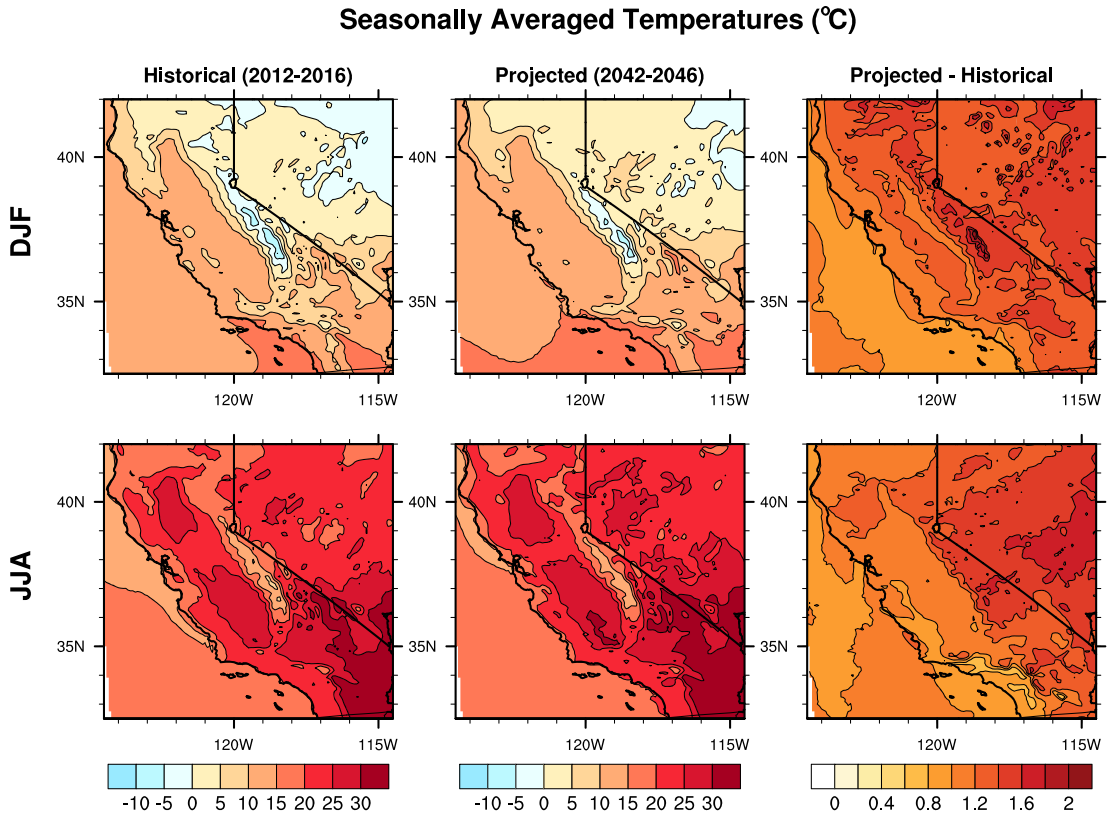

Figure 3. Average daily 2-m temperatures (in degrees Celsius) over the five simulated winter seasons (DJF) and four simulated summer seasons (JJA). DJF = December-January-February; JJA = June-July-August.

temperatures at the highest elevation over the midcentury period are pushed to approximately 2 °C over historical through the winter season.

Figure 5 depicts the number of extreme heat days per WY, defined as days where the daily maximum temperature reaches 40 °C (104 °F). Extreme temperature days are important as they are indicative of significant stress for agriculture, ecosystems, and local populations. Such days are particularly concentrated in the Central Valley and southeast desert regions which historically experience up to 30–40 and 80 days per WY, respectively. Under the influence of climate change, regions that already experience many extreme temperature days will experience more such days. Some years (particularly WY2013/2046 and WY2014/2047) produce more than 20 additional extreme temperature days per WY throughout the Tulare Basin and Sacramento Valley. The desert region of southeastern California is anticipated to become increasingly inhospitable with extreme temperature days increasing by over 30 in both WY2013/2043 and WY2014/2044. Statewide, this response appears to be more pronounced during drought years, as WY2017/2047 only experienced a modest increase of 5–10 extreme temperature days; however, further study is needed to confirm this sensitivity. Figures 3 and 5 also highlight to an important observation: regions with more extreme temperature days are not regions with the greatest increase in average temperature.

4.3. Precipitation

Figure 6 (top row) depicts average daily wintertime precipitation simulated over the historical and projected time periods (combining rain and snow, in millimeter per day). In agreement with past studies (e.g., Huang & Ullrich, 2017), total precipitation increases by approximately 5% through much of the domain, particularly throughout the Sierra Nevada, the Klamath, and along the central and northern coast. Notably, the mean change in wintertime precipitation total is largely insensitive to altitude (Figure 4c). The increase in precipitation is particularly robust in the Northern Sierra Nevada across model years, as apparent from the simulated North Sierra precipitation eight-station index (Figure 7), derived from the accumulated precipitation totals received at eight meteorological stations throughout this region (see California Department of Water Resources, 2018b). Through the Southern Sierra Nevada, the precipitation change is similarly assessed using

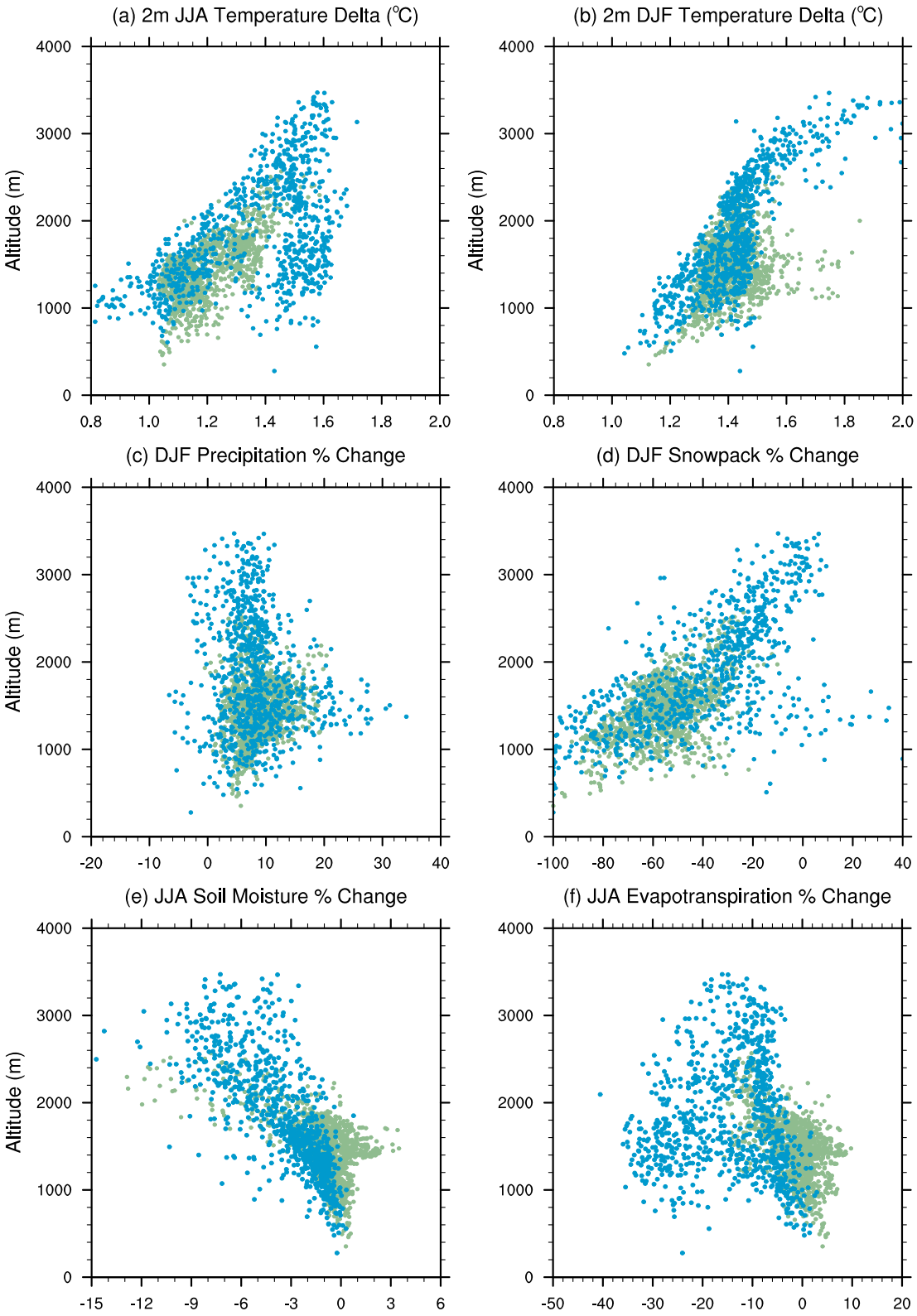

Figure 4. (a) DJF 2-m temperature difference, (b) JJA 2-m temperature difference, (c) DJF precipitation percent change, (d) DJF snow water equivalent percent change, (e) JJA soil moisture percent change, and (f) JJA evapotranspiration percent change, averaged over season and the drought period WY2012–2016, versus altitude at each model grid point in the mountain region. Blue (green) dots denote southern (northern) Sierra Nevada grid points, divided along 38.5°N. DJF = December-January-February; JJA = June-July-August.

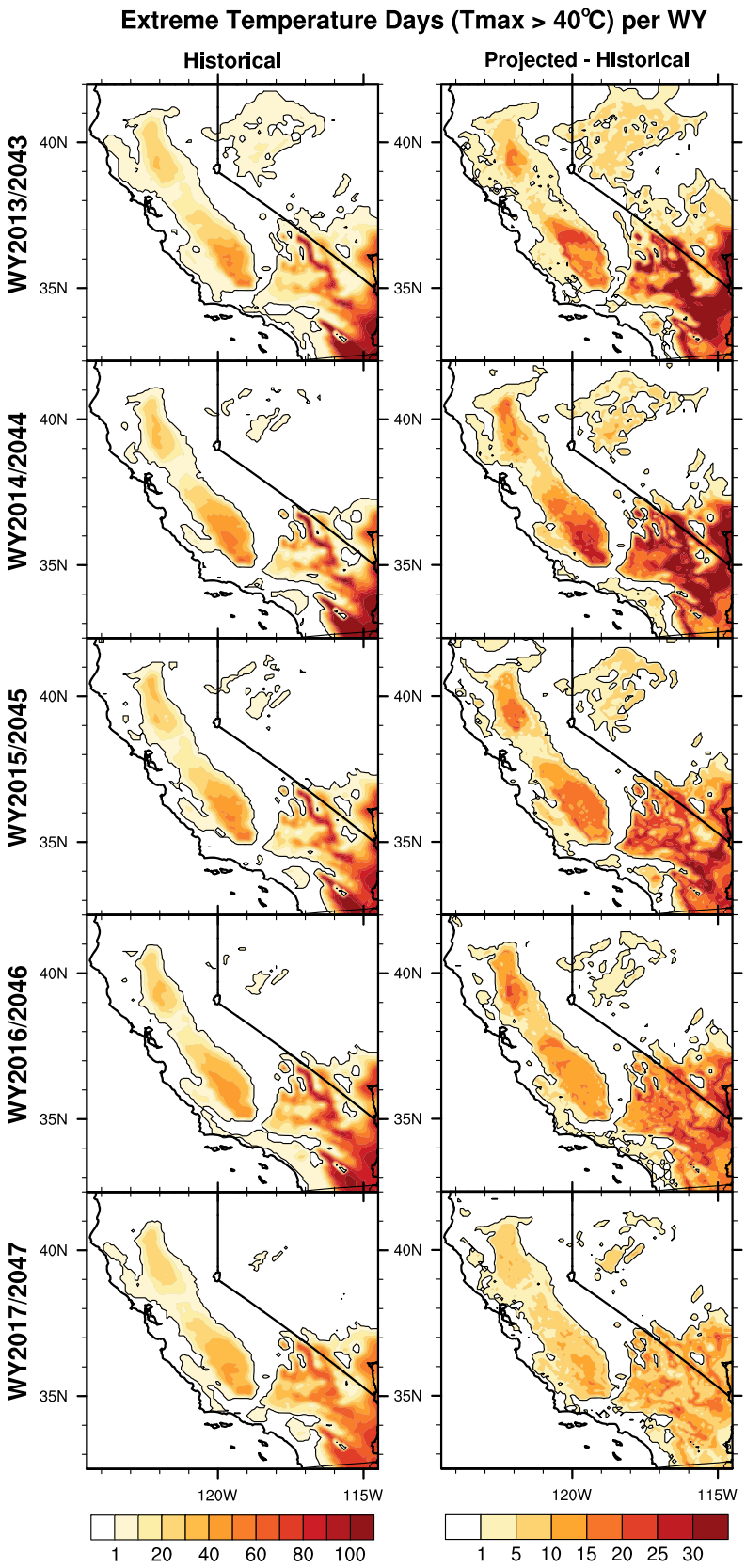

Figure 5. Historical number of extreme temperature days (those with 2-m Tmax greater than 40 °C or 104 °F) per water year and projected difference in number of extreme temperature days. WY = water year.

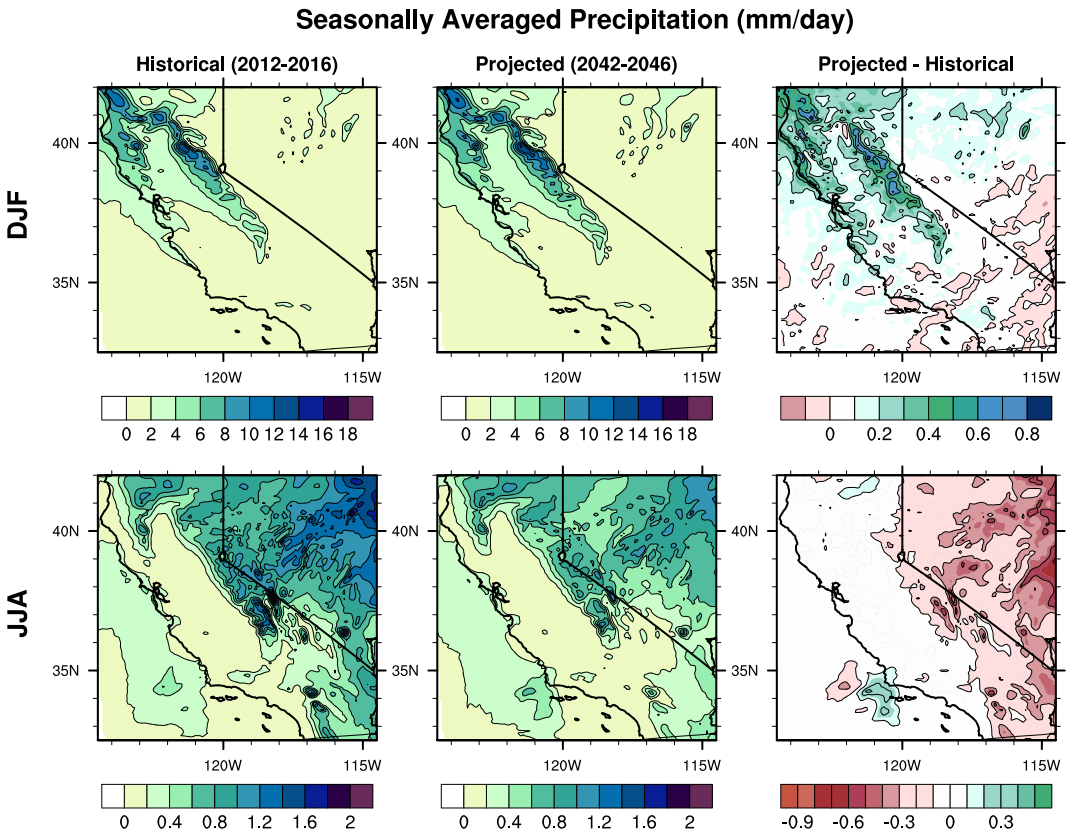

Figure 6. Average daily climatological precipitation (mm/day) over (top row) the four winter seasons (DJF) of the drought and (bottom row) the four summer seasons (JJA) of the drought and climatological difference between projected and historical precipitation. Note the difference in scales between top and bottom rows. DJF = December-January-February; JJA = June-July-August.

the Tulare Basin six-station index (Figure 7); although a 5% increase in precipitation is apparent in WY2017, for most dry years the precipitation change is far less. Further, through the southeast desert region of the State there are patches that experience a slight decrease in average wintertime precipitation on the order of <0.1 mm/day (largely coincident with the Lower Colorado watershed). In conjunction with increased temperatures in these regions we anticipate widespread wintertime drying to occur in this already dry region.

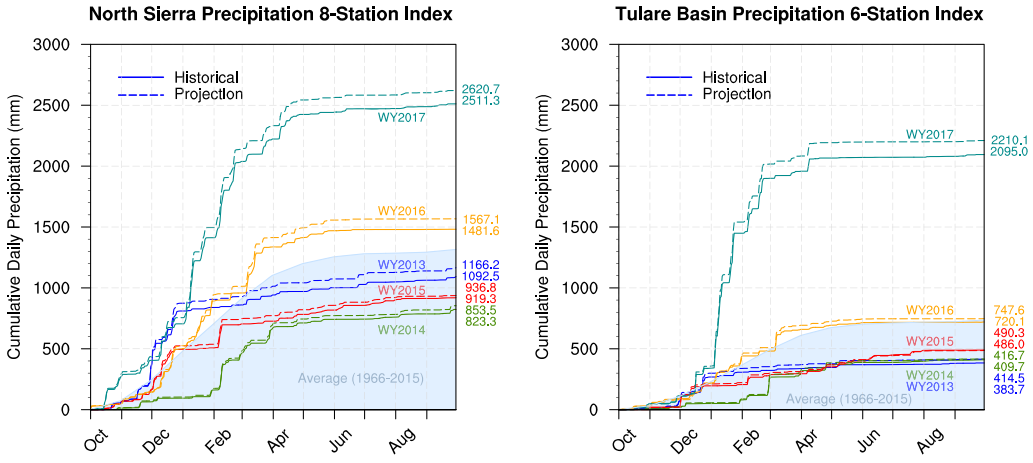

Figure 7. (left) North Sierra precipitation eight-station index and (right) Tulare Basin precipitation six-station index from simulated historical and projected drought years.

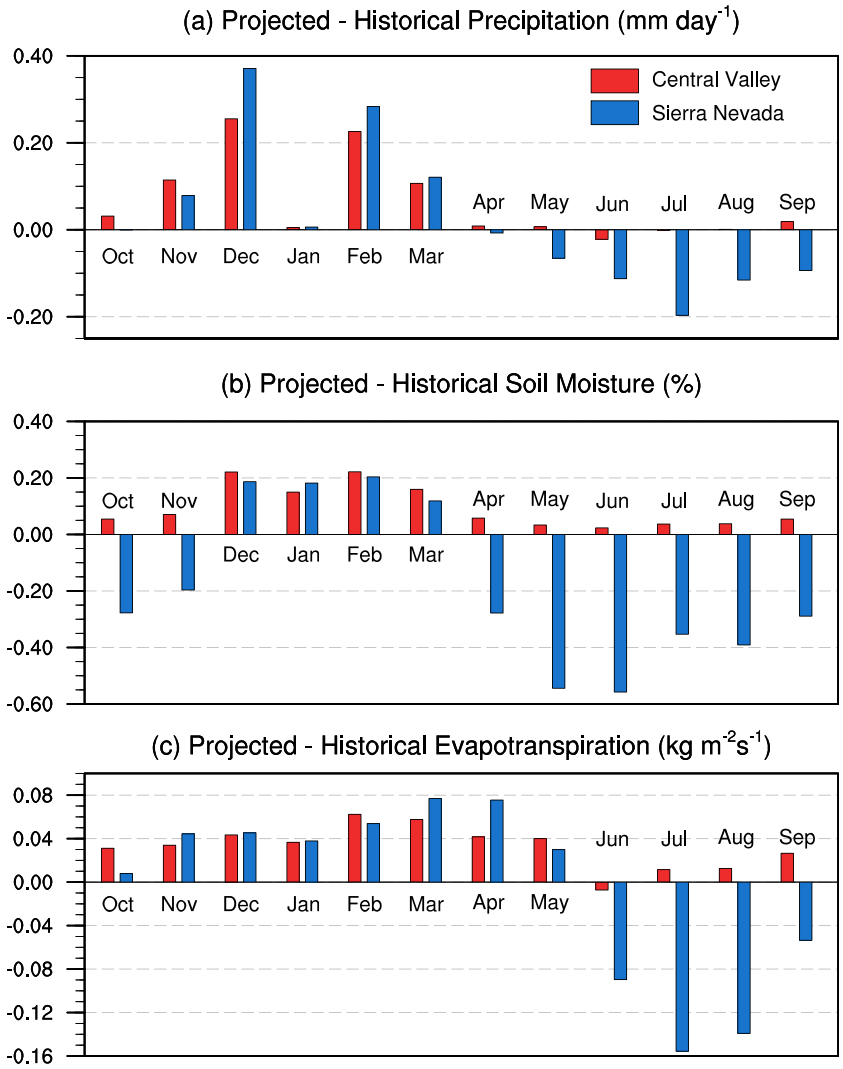

Figure 8. Absolute change future (WY2043 to WY2046) minus historical (WY2013 to WY2016) in monthly precipitation rate, soil moisture, and evapotranspiration in the Central Valley and Sierra Nevada regions.

Although summertime in the U.S. west is far drier than winter, summertime precipitation is nonetheless relevant in the mountains of California and throughout Nevada. Figure 6 (bottom row) shows that the projected drought features substantially increased inland drying over the summer season compared with the historical period. The decrease in precipitation over this period is anticipated to occur because of higher air temperatures and limited water availability, leading to a decrease in relative humidity. The moistening of the winter season and drying of the summer season is reflected clearly in the precipitation seasonality: Figure 8a depicts the absolute change in monthly precipitation over the drought period (WY2013/2043 to WY2016/2046). Note that months of January of the drought period experienced abnormally low precipitation simply as a result of storm timing, so appear as an outlier in this analysis. In general, increases in precipitation rate are concentrated in the wet period between November and March, with drying occurring at other times. A tendency toward enhanced seasonality in precipitation has also been recently pointed out by Swain et al. (2018). The drivers of this increased seasonality are theorized to be both dynamical and thermodynamical, although this study only considers the effect of the latter. A dynamical shift in jet stream position would also be relevant in enhancing the north-south gradient of wetting/drying but is not investigated in this study.

This increased precipitation variability is analogous to what has been discussed in section 3 and is further reflected in the dry and wet extremes. In Figure 9, daily precipitation amount is assessed in terms of the number of dry days (left), defined as days with precipitation less than 1 mm/day, and extreme precipitation

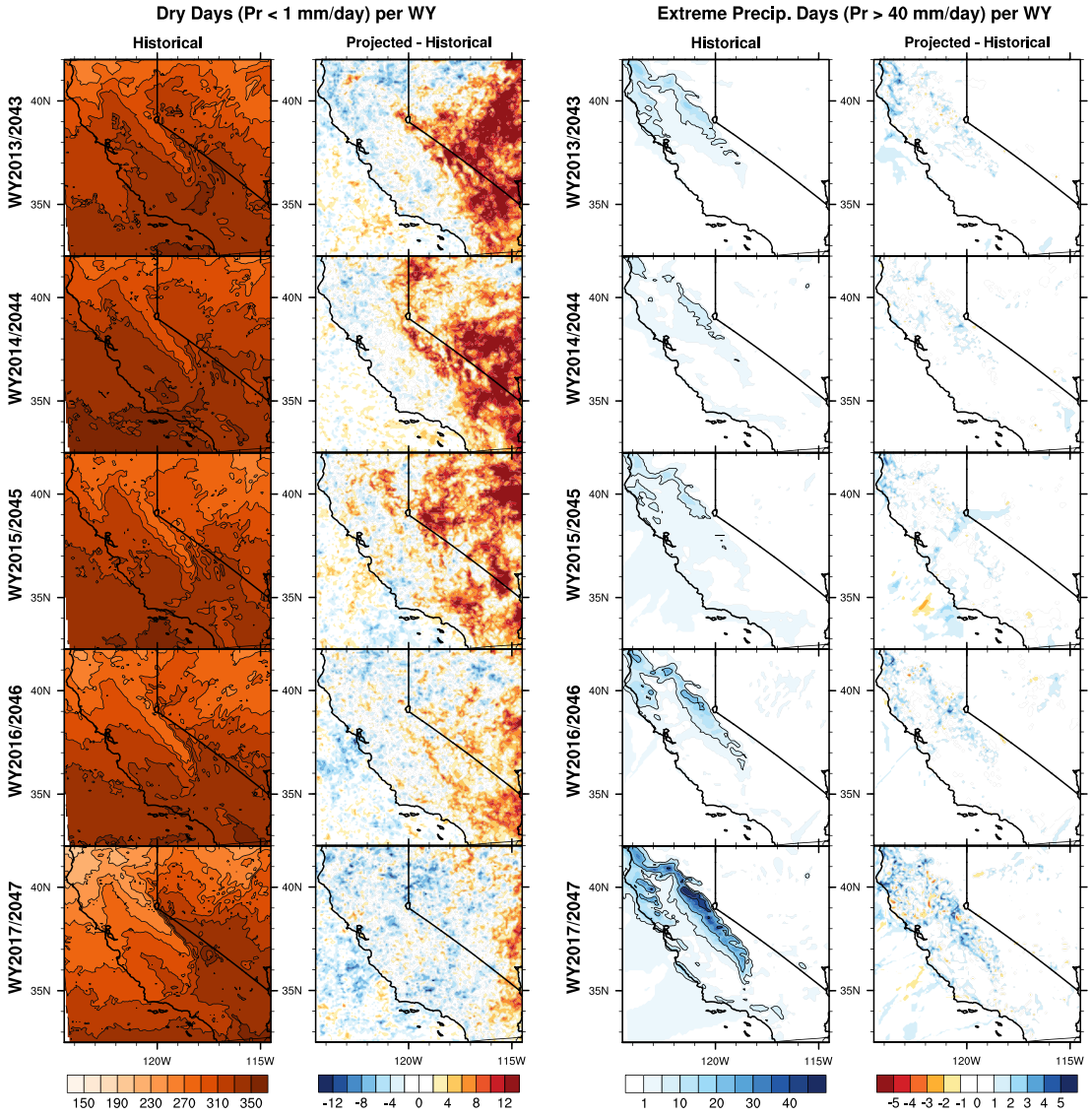

Figure 9. (left) Number of *dry days* from each water year (defined as days with precipitation less than 1 mm/day) from historical simulation and the difference between projections and historical. (right) Number of extreme precipitation days from each water year (defined as days with precipitation greater than 40 mm/day) from historical simulation and the associated difference between projections and historical. For extreme precipitation days, historical contour lines appear at 5, 20 and 40 days/WY. WY = water year.

days (right), defined as days with precipitation greater than 40 mm/day. In general, the number of historical dry days per year increases from northwest to southeast; however, the projected change in number of dry days increases from west to east, in accordance with the change in summertime precipitation exhibited in Figure 6. There is essentially no change in the number of dry days west of 120°W, a region that includes the coastal regions and the Central Valley, but an increase in dry days over the Sierra Nevada, southeastern California, and throughout Nevada. Notably, the driest years of the simulation (i.e., WY2013/2043 and WY2014/2047) also exhibit the greatest increase in the number of dry days, whereas the number of dry days in the WY2017/2047 drought buster was approximately consistent between historical and projection. There also remains a robust increase in the number of extreme precipitation days over all simulated years (see Table 2), sharing an analogous geographic pattern to mean precipitation and indicative of the increased frequency of extreme precipitation events under climate change. Overall, these results suggest that, when they occur, extreme rainfall days will be more intense than they have been historically, in agreement with past work (i.e., Huang & Ullrich, 2017).

Table 2
Average Number of Extreme Precipitation Days Along the Windward Flank of the Sierra Nevada Mountains From Each Water Year

Period	WY2013/2043	WY2014/2044	WY2015/2045	WY2016/2046	WY2017/2047
Historical	3.73	2.81	2.86	6.74	21.1
Projected	4.08	3.16	3.22	7.34	22.1

The projected changes in precipitation in this study can be succinctly summarized as *wet becomes wetter, dry becomes drier*. With that said, one should be careful to interpret *dry* and *wet* in context (Byrne & O'Gorman, 2015). Here the wintertime Sierra Nevada, exemplary of a wet season and region, exhibits increases in both mean and extreme precipitation (although this increase is tempered during the drought period). On the other hand, southeastern California, Nevada, and the summertime Sierra Nevadas exhibit increased drying that is enhanced through the drought period. The drivers for this change are largely thermodynamic, arising from higher atmospheric water vapor content, but accompanied by a higher threshold for triggering precipitation. However, secondary drivers also accompany this change in precipitation, including reduced wintertime

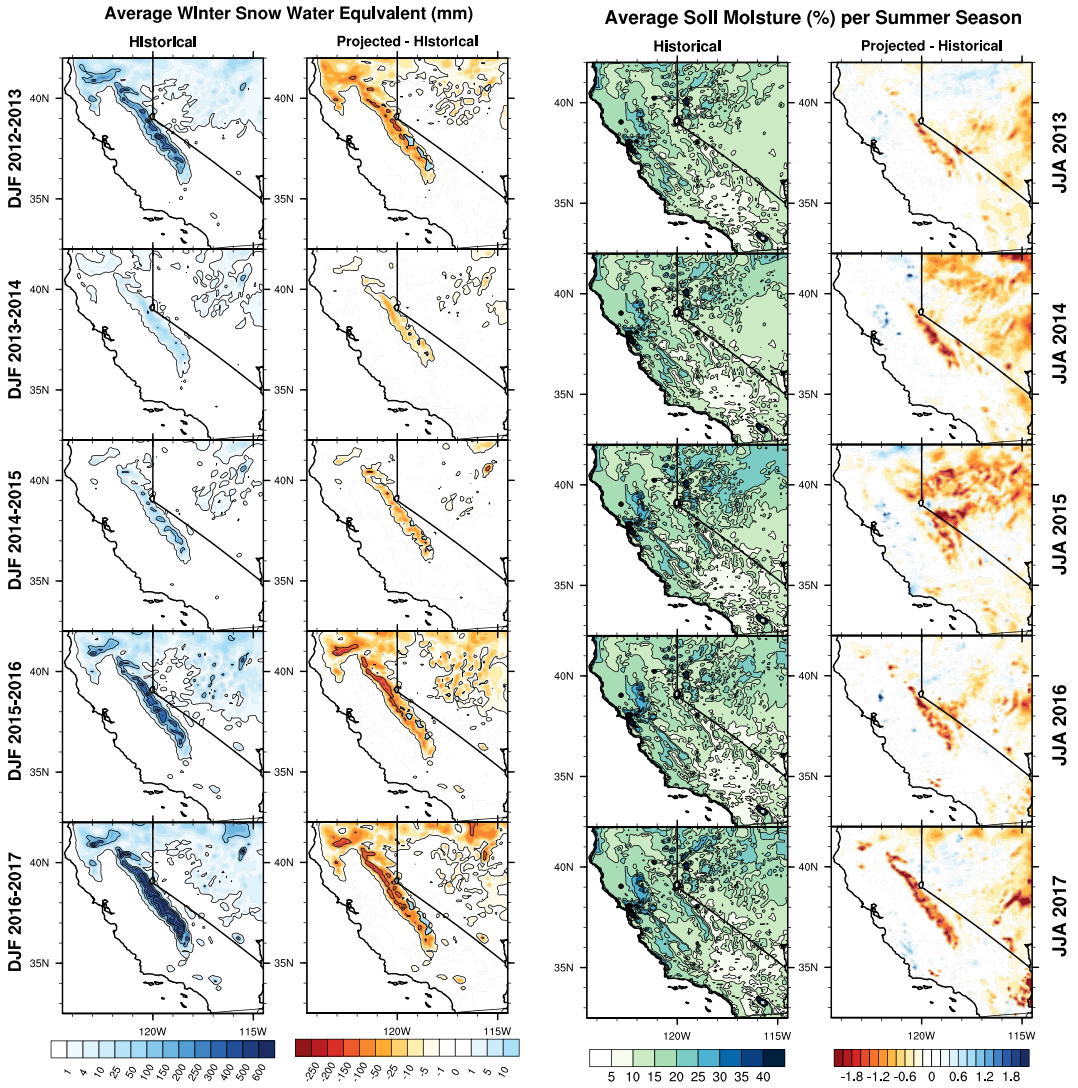

Figure 10. (first and second columns) Historical DJF SWE (mm) and SWE difference between projection and historical. (third and fourth columns) Historical soil moisture over each summer season and difference between projection and historical. DJF = December-January-February; SWE = snow water equivalent; JJA = June-July-August.

Table 3
Peak Total SWE Volumes in Million Acre-Feet for the 10 Reservoir Upstream Regions From Each Water Year

Period	WY2013/2043	WY2014/2044	WY2015/2045	WY2016/2046	WY2017/2047
Historical	6.20	2.46	1.48	7.82	14.7
Projected	5.12	1.79	1.04	5.56	12.0

Note. SWE = snow water equivalent.

snowpack volume (discussed in the next section) leading to a decrease in summertime soil moisture, ET, and hence water vapor availability.

4.4. Mountain Snowpack

The variability of Sierra Nevada snowpack from WY2013 to WY2017 was remarkable. Snowpack ranged between 5% of normal in WY2015, a 1-in-500 year event (Belmecheri et al., 2016; Margulis et al., 2016), and more than 150% of normal in WY2017. This interannual variability was also captured in historical modeled average wintertime snowpack volume (Figure 10). Strikingly, in future years significant average wintertime snow water equivalent (SWE) decline was found throughout the Sierra Nevada across all WYs, with up to 248.9 mm (9.8 in) in some regions. The decline in winter season SWE occurred at all elevations of the Sierra Nevada, especially in the north, and without regard to the relatively elevation-insensitive 5–10% increase in winter season precipitation (Figure 4d). In general, precipitation phase during a future drought tends toward more rainfall and less snowfall, due to near-surface temperature increases in regions historically at-or-near freezing (Figure 3). This has been corroborated in other climate change studies using several regional climate modeling strategies (Huang et al., 2018; Huang & Ullrich, 2017; Pierce & Cayan, 2013; Rhoades et al., 2017; Sun et al., 2016; Wehner et al., 2017).

Due to the particular importance of SWE to water supply (Dettinger & Anderson, 2015), we decompose future change in more detail using a set of regions upstream of 10 major reservoirs in California (Figure 2) and snowpack metrics from Rhoades et al. (2018). Projections of the future drought suggest that the date of peak SWE does not shift appreciably; however, peak total SWE volumes were dramatically reduced in these headwater regions. Although the date of peak SWE does not change markedly, the projected melt season does shorten across all WYs likely because of increased snow ripening. Simulated peak total SWE volume diminished between 18% and 30% across the WY2013–2016 from 18.0 MAF (1 MAF = 1.23348 km^3) to 13.5 MAF, a net loss of 4.5 MAF or 25% (Table 3). For context, 4.5 MAF represents 10% to 15% of California's total annual applied water use of 30 to 45 MAF (Mount & Hanak, 2016). This result suggests that SWE loss will be exacerbated in already dry years. Historically, WY2017 represented nearly half (14.7 MAF) of the total SWE accumulation from WY2013 to WY2017 (32.7 MAF); however, the WY2047 drought buster also provided less relief with only 12.0 MAF of SWE, an 18% decrease from WY2017. Coinciding with the substantial reduction of peak total SWE, a net decrease across the WY2013–2016 in snow season length was found (77 days). The net decrease in snow season length primarily occurred in the melt season (measured as the duration between peak SWE to 10% of peak SWE), reducing the length of the spring snowmelt pulse. This reduction in melt season length limits the historical role of spring snowmelt in buffering against summer aridity. A likely mechanism for this amplified snow loss is due to the snow-albedo feedback (Qu & Hall, 2007) which was corroborated in Berg and Hall (2017) using a similar historical drought analog WRF simulation. The snow-albedo feedback is particularly relevant at the intersection of the snow and freezing line.

Although all 10 upstream regions exhibited a net decrease in peak total SWE volume under pseudo global warming, the 7.1-MAF reduction over WY20103–2017 was not spread evenly throughout California. As the mountains of the southern Sierra Nevada are at higher elevation than the northern Sierra Nevada, this region tends to exhibit more resiliency to increased temperatures. Figure 11 highlights the simulated historical and projected peak total SWE volumes and snow season lengths for regions upstream of each reservoir. Two-thirds of the 7.1-MAF lost in our projections came from the northern reservoirs of Shasta, Oroville, and Folsom (i.e., 14.1 to 9.4 MAF). As expected, some resiliency in snowpack to warming in the future was found in the three central regions of the Sierra Nevada with Don Pedro, Exchequer, and Pine Flat reductions only at 9% to 13% (i.e., 12.2 to 10.9 MAF). This suggests that the northern reservoirs would have to manage for even less snowmelt to replenish reservoir levels than those that are more centrally located in the Sierra Nevada. Given that winter season total precipitation increased under pseudo global warming, the loss in snowpack would primarily impact the timing and not the magnitude of total runoff in the WY.

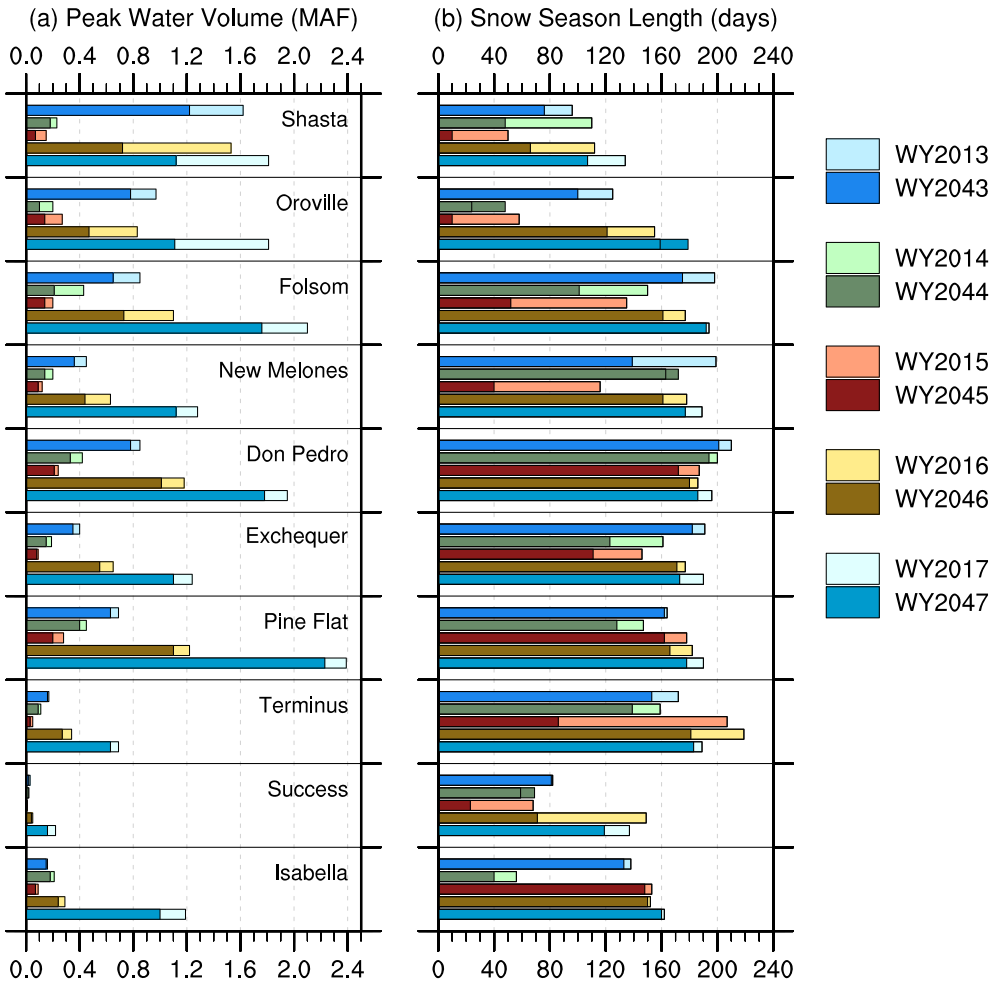

Figure 11. Simulated estimates of total water volume and snow season length for each of the 10 reservoir upstream regions (as depicted in Figure 2). MAF = million acre feet; WY = water year.

4.5. Soil Moisture

Soil moisture is a critical component of drought indices which help to inform wildfire potential and increases in water demand, particularly in summers. In WRF-CLM, the top 3.4 m of soil, represented by 10 vertical layers, is used to compute soil moisture content. Notably, our simulations did not account for irrigation. In Figure 10, a clear spatial variability of JJA soil moisture is observed across WYs. The highest soil moisture concentrations were found in the western side of the Central Valley (25% to 30%), and the driest soil concentrations were found in the Mojave Desert (<10%). A clear interannual variability was also present in simulations, particularly in southern California where soil moisture deficits lasted 3 years from JJA 2013 to 2015 but recovered in JJA 2016.

Although Sierra Nevada total wintertime precipitation increases under our future projections (Figure 8b), summertime soil moisture is consistently depleted, in part due to increases in ET and decreases in mountain snowpack and snow season duration associated with warmer temperatures in WY2043 to WY2047 (Figures 10 and 11). Decreases in summertime soil moisture were primarily found in the central Sierra Nevada and the Great Basin in Nevada (i.e., 1.5% to 2.5%), both of which are influenced by seasonal snowpack. Interestingly, even under the relatively nominal precipitation conditions of WY2016, our projections imply a decline in summer soil moisture in the central Sierra Nevada. This highlights the importance of snowmelt duration in the Sierra Nevada to counteract summer aridity. Outside of the Sierra Nevada, soil moisture differences were minimal and may be due to soil moisture already being low and/or the influence of soil porosity in nonmontane environments which induce higher retention of precipitation. However, in certain agricultural hot spots such as the Ojai and Imperial Valley soil moisture deficits over JJA 2013 to 2015 were enhanced in the future.

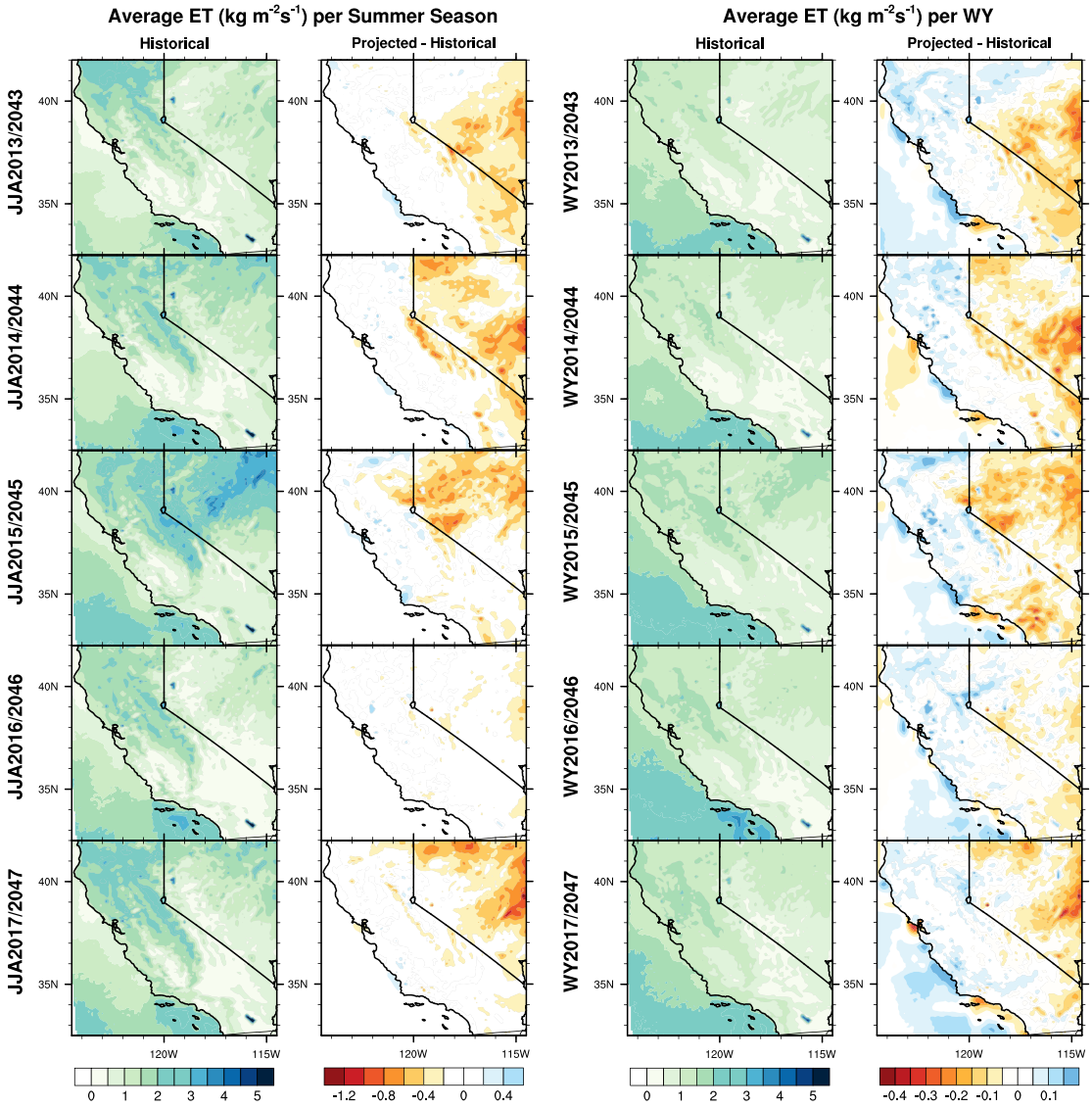

Figure 12. Historical evapotranspiration and difference between projection and historical over (first and second columns) each summer season and (third and fourth columns) each WY. WY = water year; ET = evapotranspiration; JJA = June-July-August.

Without added irrigation (likely drawn from groundwater stores), agricultural productivity in these two regions would be further impacted. Our study did not consider the regional climate effects of changes in agricultural irrigation practices that might result from decreased water availability. Reductions in agricultural irrigation could result in lower soil moisture and ET, as well as increased surface air temperatures (Huang & Ullrich, 2016).

The elevation dependence of soil moisture (Figure 4e) further reflects the detrimental impacts of snowpack loss and elevation-dependent warming to soil moisture. These results indicate that the greatest relative change in soil moisture occurs above 1,800 m, where the combined effect of temperature and snowpack loss are most pronounced.

4.6. ET and Water Demand

Drought is fundamentally an imbalance between water supply and demand — both of which can be impacted by a changing climate. On the demand side, irrigation requirements are closely linked to ET, which is itself controlled by atmospheric demand factors such as relative humidity, turbulence, and radiation, as well as available soil moisture. Enhanced ET in upper watershed regions can also reduce the amount of precipitation that contributes to streamflow and hence to the water supply. Comparing projections with historical, there

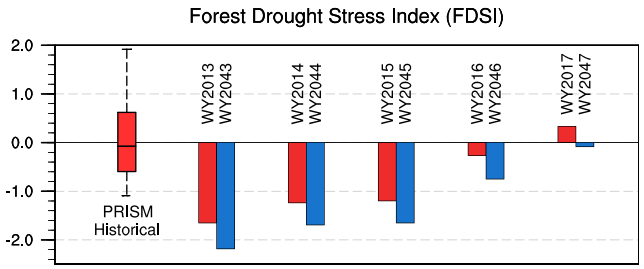

Figure 13. Bias-corrected forest drought stress index (FDSI) for each water year of the analysis period and PRISM-derived 1981–2012 historical index values. The bias-corrected values were computed as ⟨PRISM Historical FDSI⟩ + ⟨WRF Projected FDSI⟩ − ⟨WRF Projected FDSI⟩.

is a general increase in the annual ET rates throughout the drought years (Figure 12). The most noticeable increases occur over the central coast, north coast, and central valley of up to 5.4%, 4.8%, and 3.9%, respectively. ET increases over open water, where soil moisture is not a limiting factor, provide evidence for higher atmospheric water demand in the future. The ET response to warming during the summertime, however, is more complicated and entangled with fluctuations of soil moisture and precipitation. The Central Valley experiences only a small (<1.3%) increase in ET as ET is limited by the soil moisture. The Sierra Nevada region, on the other hand, experiences an average 8.3% decrease in ET, a result of reduced warm-season precipitation, snowpack, and therefore available soil moisture content in this area during the summer months. Figure 4f demonstrates the altitude dependence of summertime ET change through the mountains, with decreases of up to 40% in ET through much of the southern Sierra Nevada. The impacts on ET from climate change are much more pronounced in this region, particularly between 1,000 and 2,000 m where we anticipate the greatest recession of the snowpack.

The simulated changes in ET rates are highly seasonal (Figure 8c). Over the Central Valley and Sierra Nevada, the ET rates are increased (up to 7.7% and 9.0%, respectively) during the months of October through May, when the baseline soil moisture content is relatively high. However, the ET rates either decrease or are unchanged in the face of the projected warming during the drier months of June through September. The increases in precipitation rates during the wet months provide extra soil moisture explaining the increases in the ET during these months. However, the fact that the elevated ET rates outlast the increases in precipitation and the soil moisture content shows that the warming trends also play a role in the increased ET rates. However, the higher temperatures not only stop being effective in elevating ET once the soil moisture reaches the minimum level in June but also exhaust soil moisture content faster which results in decreases in ET rates over the dry summer months, particularly over the Sierra Nevada.

Note that these simulations do not account for irrigation water applied to agricultural and urban areas of California. If soil moisture content is maintained via irrigation, we speculate that the ET increases would intensify throughout the summer months which imply meaningful increases in water demands in the agricultural and urban regions in the Central Valley. However, more investigation is needed to make certain conclusions about the effects of a warming climate on the ET rates and therefore water demands over irrigated regions in California. Furthermore, it is important to note that this study uses the same vegetation dynamics for the historical and projected scenarios. This means that the potential response of vegetation to the changes in atmospheric conditions such as temperature, humidity, and CO_2 concentration or soil moisture is not taken into account.

4.7. Impacts on the Forests of the Sierra Nevada

The impacts of climate change on the drought described so far have obvious repercussions for water resource management, human populations, and ecosystems, to give a few examples. In this section we focus on the forests of the Sierra Nevada, which were critically altered over the historical drought period. To quantitatively understand the impacts of a future drought, forest drought stress index (FDSI) has been derived to evaluate the declines of tree productivity and survival by drought in a long-term climate change trend. Specifically, this index is calculated as a combination of the previous warm-season August–October and growing-season May–July vapor pressure deficit and cold-season precipitation (Williams et al., 2013). Negative values of this quantity are particularly indicative of forest stress and correlate well with losses of forest acreage due to insufficient water availability, forest fire, and destruction by invasive pests (such as bark beetle). Monthly PRISM data (Daly et al., 2008) for precipitation, average dew point and surface temperature from 1981 to 2017, are standardized to compute the long-term FDSI, as well as the indices for historical and projection simulations. FDSI is only calculated in the Sierra Nevada Region where forest is the major land cover category.

In Figure 13, the historical range of FDSI indices (1981–2012) is reflective of wet and dry years that have occurred over this period. Over the historical drought period, FDSI values are negative from 2012 to 2016 but recovering to positive in WY2017. The negative FDSI implies less precipitation during winter season and significant vapor pressure deficit caused by higher temperature. Future projections have even smaller FDSI

values (by ~0.5 or about one standard deviation of historical FDSI values), indicating higher modality of trees when a drought occurs in the middle of this century. The 2012–2016 period featured 3 years with FDSI values below the minimum historical value from Parameter-elevation Regressions on Independent Slopes Model (PRISM), associated with a loss of 102 million trees across California (as reported by the U.S. Forest Service). Our midcentury drought scenario promises a dramatic worsening of this impact, with unprecedented low values of FDSI.

5. Summary and Conclusions

In this paper, a midcentury (2042–2047) drought scenario is presented that is closely modeled after the record-breaking historical California drought and subsequent relief period (2012–2017). Forcing from climate change is imposed by modifying the lateral boundary conditions, greenhouse gas forcing, and sea surface temperatures within a regional climate model framework (WRF). Using global climate model simulations from CMIP5 to guide these modifications, the dynamical conditions of the historical drought period are retained but subjected to the modified thermodynamic conditions of the midcentury period. Given that the greatest uncertainties from climate change are from its implications for planetary dynamics, the pseudo global warming approach allows us to avoid these uncertainties and focus on the dominant thermodynamic drivers. Overall, climate change greatly exacerbates the historical drought period, with significantly more extreme heat days, record-low snowpack, increased soil drying, and record-high forest mortality. In particular, the key differences between the historical drought period and midcentury drought period are as follows:

1. Midcentury temperatures increase by 0.8–1.4 °C (1.4–2.0 °F) in the Central Valley and 1.2–2.0 °C (2.2–3.6 °F) in the mountainous regions and interior. Greater temperature increases are expected at higher altitudes due to elevation-dependent warming feedbacks associated with snowpack loss.
2. The number of extreme temperature days per WY (those with temperatures greater than 40 °C or 104 °F) increase by 5–20 in the north Central Valley (from 10 to 40 per year), by 10–25 in the Tulare basin (from 20 to 40), and by 15–30 (from 50 to 90) in the southeastern desert region. The greatest increase in extreme temperature days occurred in years that are already dry.
3. Average WY precipitation along the windward flank of the Sierra Nevada and in the Klamath increases by approximately 5% across all years. Southern California and the southeast desert region see no significant change in average precipitation. These changes in precipitation primarily occur because of an enhancement in total precipitation per precipitation event.
4. The number of dry days per WY (those with <1 mm/day of total precipitation) consistently increases by 6–12 in the mountain region, through the Great Basin and through the southeastern desert region.
5. The number of extreme precipitation days (those with >40 mm/day of total precipitation) through the mountain region increases by 0.5 in dry years and by 1 in WY2017 (spatially averaged).
6. Peak total SWE water volume diminishes between 16% and 30% across the five WYs from 32.6 to 25.5 MAF, a net loss of 7.1 MAF or 22%.
7. Two-thirds of the 7.1 MAF lost occurred in Shasta, Oroville, and Folsom (i.e., 14.1 to 9.4 MAF). Some resiliency in snowpack to warming in WY2043 to WY2046 is found in the three central regions of the Sierra Nevada with Don Pedro, Exchequer, and Pine Flat reductions only at 9% to 13% (i.e., 12.2 to 10.9 MAF).
8. Average JJA soil moisture in dry years reduces by 1–2% at higher elevations (typically 10–20%) and 0.5–1% in other high-elevation regions and through Southern California. No significant change in summertime soil moisture occurred elsewhere in the domain or during WY2017/2047.
9. In response to lower soil moisture conditions and reduced snowpack, ET drops in the Sierra Nevadas and through the Great Basin.
10. The FDSI drops by about 0.5 in the future drought period, indicative of record-high stress on the forests of the Sierra Nevada.

Given that the dynamical conditions associated with the 2012–2016 drought are likely to increase in frequency in the coming century, this study provides a means to structure future drought planning around a drought scenario that is realistic and modeled after a memorable historical analog. In particular, we highlight regional changes in temperature, precipitation, snowpack and forest health with clear and deleterious impacts for water management, groundwater sustainability, rural communities, and ecosystem maintenance. To instill adaptive resiliency to such a drought, stakeholders, water managers, and government agencies, at all levels, will need to begin the process of coordination and preparation now to ensure that they can overcome these substantial challenges when they occur.

Acknowledgments
The authors would like to thank Amy Yu and two anonymous reviewers for their comments and suggestions. This publication was developed with partial support from Assistance Agreement 83586701 awarded by the U.S. Environmental Protection Agency to the Public Policy Institute of California. It has not been formally reviewed by EPA. The views expressed in this document are solely those of the authors and do not necessarily reflect those of the agency. EPA does not endorse any products or commercial services mentioned in this publication. Authors Jones, Rhoades, and Ullrich were supported by the Department of Energy Office of Science award DE-SC0016605, *An Integrated Evaluation of the Simulated Hydroclimate System of the Continental United States*. This project is also supported by the National Institute of Food and Agriculture, U.S. Department of Agriculture, hatch project under California Agricultural Experiment Station project CA-D-LAW-2203-H. This research used resources of the National Energy Research Scientific Computing Center, a DOE Office of Science User Facility supported by the Office of Science of the U.S. Department of Energy under contract DE-AC02-05CH11231. The WRF model output used in our analysis is available from ZENODO at https://doi.org/10.5281/zenodo.1340743.

References

AghaKouchak, A, Cheng, L., Mazdiyasni, O., & Farahmand, A. (2014). Global warming and changes in risk of concurrent climate extremes: Insights from the 2014 California drought. *Geophysical Research Letters*, *41*, 8847–8852. https://doi.org/10.1002/2014GL062308

Asner, G. P., Martin, R. E., Anderson, C. B., & Knapp, D. E. (2015). Quantifying forest canopy traits: Imaging spectroscopy versus field survey. *Remote Sensing of Environment*, *158*, 15–27. https://doi.org/10.1016/j.rse.2014.11.011

Ault, T. R., Cole, J. E., Overpeck, J. T., Pederson, G. T., & Meko, D. M. (2014). Assessing the risk of persistent drought using climate model simulations and paleoclimate data. *Journal of Climate*, *27*(20), 7529–7549. https://doi.org/10.1175/JCLI-D-12-00282.1

Belmecheri, S., Babst, F., Wahl, E. R., Stahle, D. W., & Trouet, V. (2016). Multi-century evaluation of Sierra Nevada snowpack. *Nature Climate Change*, *6*(1), 2–3. https://doi.org/10.1038/nclimate2809

Berg, N., & Hall, A. (2017). Anthropogenic warming impacts on California snowpack during drought. *Geophysical Research Letters*, *44*, 2511–2518. https://doi.org/10.1002/2016GL072104

Borsa, A. A., Agnew, D. C., & Cayan, D. R. (2014). Ongoing drought-induced uplift in the western United States. *Science*, *345*(6204), 1587–1590. https://doi.org/10.1126/science.1260279

Bretherton, C. S., & Park, S. (2009). A new moist turbulence parameterization in the community atmosphere model. *Journal of Climate*, *22*(12), 3422–3448. https://doi.org/10.1175/2008JCLI2556.1

Byrne, M. P., & O'Gorman, P. A. (2015). The response of precipitation minus evapotranspiration to climate warming: Why the "wet-get-wetter, dry-get-drier" scaling does not hold over land. *Journal of Climate*, *28*(20), 8078–8092. https://doi.org/10.1175/JCLI-D-15-0369.1

California Climate Change Technical Advisory Group (CCTAG) (2015). Perspectives and guidance for climate change analysis: California department of water resources technical information record. California DWR Climate Change Technical Advisory Group. Retrieved from http://www.water.ca.gov/climatechange/docs/2015/Perspectives_Guidance_Climate_Change_Analysis.pdf

Cai, W., Borlace, S., Lengaigne, M., Van Rensch, P., Collins, M., Vecchi, G., et al. (2014). Increasing frequency of extreme El Niño events due to greenhouse warming. *Nature Climate Change*, *4*(2), 111. https://doi.org/10.1038/nclimate2100

Caldwell, P., Chin, H.-N. S., Bader, D. C., & Bala, G. (2009). Evaluation of a WRF dynamical downscaling simulation over California. *Climatic Change*, *95*(3-4), 499–521. https://doi.org/10.1007/s10584-009-9583-5

California Department of Food and Agriculture (2016). California Agricultural Statistics Review: 2016-2017. Retrieved from https://www.cdfa.ca.gov/Statistics/PDFs/2016-17AgReport.pdf

California Department of Water Resources (2018a). Dayflow. Retrieved from https://water.ca.gov/Programs/Environmental-Services/Compliance-Monitoring-And-Assessment/Dayflow-Data, Accessed September 4, 2018.

California Department of Water Resources (2018b). Northern Sierra 8-Station Index. https://cdec.water.ca.gov, Accessed July 5, 2018

California Energy Commission (2018). California hydroelectric statistics & data. Retrieved from http://www.energy.ca.gov/almanac/renewables_data/hydro/, Accessed September 4, 2018.

Cook, B. I., Ault, T. R., & Smerdon, J. E. (2015). Unprecedented 21st century drought risk in the American Southwest and Central Plains. *Science Advances*, *1*(1), e1400082. https://doi.org/10.1126/sciadv.1400082

Cvijanovic, I., Santer, B. D., Bonfils, Céline, Lucas, D. D., Chiang, J. C, & Zimmerman, S. (2017). Future loss of Arctic sea-ice cover could drive a substantial decrease in California's rainfall. *Nature Communications*, *8*(1), 1947. https://doi.org/10.1038/s41467-017-01907-4

Daly, C., Halbleib, M., Smith, J. I., Gibson, W. P., Doggett, M. K., Taylor, G. H., et al. (2008). Physiographically sensitive mapping of climatological temperature and precipitation across the conterminous United States. *International Journal of Climatology*, *28*(15), 2031–2064. https://doi.org/10.1002/joc.1688

Dettinger, M. D. (2013). Atmospheric rivers as drought busters on the US West Coast. *Journal of Hydrometeorology*, *14*(6), 1721–1732. https://doi.org/10.1175/JHM-D-13-02.1

Dettinger, M. D., & Anderson, M. L. (2015). Storage in California's reservoirs and snowpack in this time of drought. *San Francisco Estuary and Watershed Science*, *13*(2), 1–5. https://doi.org/10.15447/sfews.2015v13iss2art1

Dettinger, M. D., Anderson, J., Anderson, M., Brown, L. R., Cayan, D., & Maurer, E. (2016). Climate change and the delta. *San Francisco Estuary and Watershed Science*, *14*(3). https://doi.org/10.15447/sfews.2016v14iss3art5

Funk, C., Hoell, A., & Stone, D. (2014). Examining the contribution of the observed global warming trend to the California droughts of 2012/13 and 2013/14. *Bulletin of the American Meteorological Society*, *95*(9), S11. https://doi.org/10.1175/1520-0477-95.9.S1.1

Hanak, E., Chappelle, C., Escriva-Bou, A., Gray, B., Jezdimirovic, J., McCann, H., & Mount, J. (2017). Priorities for California's water. *Public Policy Institute of California (PPIC) Water Policy Center*, 1–19. Retrieved from http://www.ppic.org/wp-content/uploads/r_1017ehr.pdf

Harpold, A., Dettinger, M., & Rajagopal, S. (2017). Defining snow drought and why it matters. *EOS-Earth & Space Science News*, *98*. https://doi.org/10.1029/2017EO068775

Held, I. M., & Soden, B. J. (2006). Robust responses of the hydrological cycle to global warming. *Journal of Climate*, *19*(21), 5686–5699. https://doi.org/10.1175/JCLI3990.1

Huang, X., Hall, A. D., & Berg, N. (2018). Anthropogenic warming impacts on today's Sierra Nevada snowpack and flood risk. *Geophysical Research Letters*, *45*, 6215–6222. https://doi.org/10.1029/2018GL077432

Huang, X., Rhoades, A. M., Ullrich, P. A., & Zarzycki, C. M. (2016). An evaluation of the variable-resolution CESM for modeling California's climate. *Journal of Advances in Modeling Earth Systems*, *8*, 345–369. https://doi.org/10.1002/2015MS000559

Huang, X., & Ullrich, P. A. (2016). Irrigation impacts on California's climate with the variable-resolution CESM. *Journal of Advances in Modeling Earth Systems*, *8*, 1151–1163. https://doi.org/10.1002/2016MS000656

Huang, X., & Ullrich, P. A. (2017). The changing character of twenty-first-century precipitation over the Western United States in the variable-resolution CESM. *Journal of Climate*, *30*(18), 7555–7575. https://doi.org/10.1175/JCLI-D-16-0673.1

Iacono, M. J., Delamere, J. S., Mlawer, E. J., Shephard, M. W., Clough, S. A., & Collins, W. D. (2008). Radiative forcing by long-lived greenhouse gases: Calculations with the AER radiative transfer models. *Jour\uline{}nal of Geophysical Research*, *113*, D13103. https://doi.org/0.1029/2008JD009944

Jiménez, P. A., Dudhia, J., González-Rouco, J. F., Navarro, J., Montávez, J. P., & García-Bustamante, E. (2012). A revised scheme for the WRF surface layer formulation. *Monthly Weather Review*, *140*(3), 898–918. https://doi.org/10.1175/MWR-D-11-00056.1

Kalnay, E., Kanamitsu, M., Kistler, R., Collins, W., Deaven, D., Gandin, L., et al. (1996). The NCEP/NCAR 40-year reanalysis project. *Bulletin of the American meteorological Society*, *77*(3), 437–471. https://doi.org/10.1175/1520-0477(1996)077h0437:TNYRPi2.0.CO;2

Kimura, F., & Kitoh, A. (2007). Downscaling by pseudo global warming method. ICCAP Final Rep., Research Institute for Humanity and Nature, Kyoto, Japan, 43–46.

Margulis, S. A., Cortes, G., Girotto, M., Huning, L. S., Li, D., & Durand, M. (2016). Characterizing the extreme 2015 snowpack deficit in the Sierra Nevada (USA) and the implications for drought recovery. *Geophysical Research Letters*, *43*, 6341–6349. https://doi.org/10.1002/2016GL068520

Mount, J., & Hanak, E. (2016). Water use in California. Public Policy Institute of California Water Policy Center , Just the FACTS. Retrieved from http://www.ppic.org/publication/water-use-in-california/

National Oceanic and Atmospheric Administration/National Centers for Environmental Information (2018). Climate at a glance: Statewide time series. National Centers for Environmental information, published August 2018, retrieved on August 31, 2018 from https://www.ncdc.noaa.gov/cag/

National Oceanic and Atmospheric Administration (2018). Climate Data Online (CDO). Retrieved from https://www7.ncdc.noaa.gov/CDO/CDODivisionalSelect.jsp, accessed July 5, 2018.

Neale, R. B., Chen, C.-C., Gettelman, A., Lauritzen, P. H., Park, S., Williamson, D. L., et al. (2010). Description of the NCAR community atmosphere model (CAM 5.0) (NCAR Tech. Note NCAR/TN-486+ STR). Boulder, Colorado: NCAR. Retrieved from https://www.ccsm.ucar.edu/models/ccsm4.0/cam/docs/description/cam4_desc.pdf

Oleson, K. W., Lawrence, D. M., Gordon, B., Flanner, M. G., Kluzek, E., Peter, J., et al. (2010). Technical description of version 4.0 of the Community Land Model (CLM) (*Tech. Rep.*) Boulder, Colorado: NCAR. https://doi.org/10.5065/D6FB50WZ

Paek, H., Yu, J.-Y., & Qian, C. (2017). Why were the 2015/2016 and 1997/1998 extreme El Niños different? *Geophysical Research Letters*, *44*, 1848–1856. https://doi.org/10.1002/2016GL071515

Palmer, W. C. (1965). Meteorological drought (Research Paper No. 45). Washington, DC: Department of Commerce.

Pepin, N., Bradley, R. S., Diaz, H. F., Baraër, M., Caceres, E. B., Forsythe, N., et al. (2015). Elevation-dependent warming in mountain regions of the world. *Nature Climate Change*, *5*(5), 424. https://doi.org/10.1038/nclimate2563

Pierce, D. W., & Cayan, D. R. (2013). The uneven response of different snow measures to human-induced climate warming. *Journal of Climate*, *26*, 4148–4167. https://doi.org/10.1175/JCLI-D-12-00534.1

Pierce, D. W., Cayan, D. R., Das, T., Maurer, E. P., Miller, N. L., Bao, Y., et al. (2013). The key role of heavy precipitation events in climate model disagreements of future annual precipitation changes in California. *Journal of Climate*, *26*(16), 5879–5896. https://doi.org/10.1175/JCLI-D-12-00766.1

Polade, S. D., Pierce, D. W., Cayan, D. R., Gershunov, A., & Dettinger, M. D. (2014). The key role of dry days in changing regional climate and precipitation regimes. *Scientific Reports*, *4*, 4364. https://doi.org/10.1038/srep04364

Prein, A. F., Holland, G. J., Rasmussen, R. M., Clark, M. P., & Tye, M. R. (2016). Running dry: The U.S. Southwest's drift into a drier climate state. *Geophysical Research Letters*, *43*, 1272–1279. https://doi.org/10.1002/2015GL066727

Qu, X., & Hall, A. (2007). What controls the strength of snow-albedo feedback? *Journal of Climate*, *20*(15), 3971–3981. https://doi.org/10.1175/JCLI4186.1

Rhoades, A. M., Huang, X., Ullrich, P. A., & Zarzycki, C. M. (2016). Characterizing Sierra Nevada snowpack using variable-resolution CESM. *Journal of Applied Meteorology and Climatology*, *55*(1), 173–196. https://doi.org/10.1175/JAMC-D-15-0156.1

Rhoades, A. M., Jones, A. D., & Ullrich, P. A. (2018). Assessing mountains as natural reservoirs with a multi-metric framework. *Earth's Future*, *6*, 1221–1241. https://doi.org/10.1002/2017EF000789

Rhoades, A. M., Ullrich, P. A., & Zarzycki, C. M. (2017). Projecting 21st century snowpack trends in western USA mountains using variable-resolution CESM. *Climate Dynamics*, *50*(1-2), 261–288. https://doi.org/10.1007/s00382-017-3606-0

Scanlon, B. R., Faunt, C. C., Longuevergne, L., Reedy, R. C., Alley, W. M., McGuire, V. L., & McMahon, P. B. (2012). Groundwater depletion and sustainability of irrigation in the US high plains and central valley. *Proceedings of the National Academy of Sciences*, *109*(24), 9320–9325. https://doi.org/10.1073/pnas.1200311109

Sewall, J. O., & Sloan, L. C. (2004). Disappearing Arctic sea ice reduces available water in the American west. *Geophysical Research Letters*, *31*, L06209. https://doi.org/1029/2003GL019133

Skamarock, W. C., Klemp, J. B., Dudhia, J., Gill, D. O., Barker, D. M., Wang, W., & Powers, J. G. (2005). A description of the advanced research WRF version 2 (*DTIC Document*). Boulder, CO: National center for atmospheric research boulder co mesoscale and microscale meteorology div. https://doi.org/10.5065/D68S4MVH

Sun, F., Hall, A., Schwartz, M., B.Walton, D., & Berg, N. (2016). Twenty-first-century snowfall and snowpack changes over the Southern California mountains. *Journal of Climate*, *29*(1), 91–110. https://doi.org/10.1175/JCLI-D-15-0199.1

Swain, D. L., Langenbrunner, B., Neelin, J. D., & Hall, A. (2018). Increasing precipitation volatility in twenty-first-century California. *Nature Climate Change*, *8*(5), 427. https://doi.org/10.1038/s41558-018-0140-y

Swain, D. L., Tsiang, M., Haugen, M., Singh, D., Charland, A., Rajaratnam, B., & Diffenbaugh, N. S. (2014). The extraordinary California drought of 2013/2014: Character, context, and the role of climate change. *Bulletin of the American Meteorological Society*, *95*(9), S3–S7.

Teng, H., & Branstator, G. (2017). Causes of extreme ridges that induce California droughts. *Journal of Climate*, *30*(4), 1477–1492. https://doi.org/10.1175/JCLI-D-16-0524.1

Trenberth, K. E. (2011). Changes in precipitation with climate change. *Climate Research*, *47*(1-2), 123–138. https://doi.org/10.3354/cr00953

Ullrich, P. A., Xu, Z., Rhoades, A., Dettinger, M. D., Mount, J. F., Jones, A. D., & Vahmani, P. (2018). California's drought of the future: A midcentury recreation of the exceptional conditions of 2012-2017: Data v1.0. http://doi.org/10.5281/zenodo.1340743

Wang, S., Anichowski, A., Tippett, M. K., & Sobel, A. H. (2017). Seasonal noise versus subseasonal signal: Forecasts of California precipitation during the unusual winters of 2015–2016 and 2016–2017. *Geophysical Research Letters*, *44*, 9513–9520. https://doi.org/10.1002/2017GL075052

Wang, S.-Y., Hipps, L., Gillies, R. R., & Yoon, J.-H. (2014). Probable causes of the abnormal ridge accompanying the 2013–2014 California drought: ENSO precursor and anthropogenic warming footprint. *Geophysical Research Letters*, *41*, 3220–3226. https://doi.org/10.1002/2014GL059748

Wehner, M. F., Arnold, J. R., Knutson, T., Kunkel, K. E., & LeGrande, A. N. (2017). Droughts, floods, and wildfires, *Climate Science Special Report: Fourth National Climate Assessment* (Vol. 1, pp. 231–256). Washington, DC: U.S. Global Change Research Program. https://doi.org/10.7930/J0CJ8BNN

Williams, A. P., Allen, C. D., Macalady, A. K., Griffin, D., Woodhouse, C. A., Meko, D. M., et al. (2013). Temperature as a potent driver of regional forest drought stress and tree mortality. *Nature Climate Change*, *3*(3), 292. https://doi.org/10.1038/nclimate1693

Williams, A. P., Seager, R., Abatzoglou, J. T., Cook, B. I., Smerdon, J. E., & Cook, E. R. (2015). Contribution of anthropogenic warming to California drought during 2012–2014. *Geophysical Research Letters*, *42*, 6819–6828. https://doi.org/10.1002/2015GL064924

Zhang, G. J., & McFarlane, N. A. (1995). Role of convective scale momentum transport in climate simulation. *Journal of Geophysical Research*, *100*(D1), 1417–1426. https://doi.org/10.1029/94JD02519